

# A generic mechanism for spatiotemporal intermittency

M. Argentina, P. Coulet\*

*INLN, UMR CNRS 129, 1361 Route des Lucioles, 06560 Valbonne, France*

---

## Abstract

A simple mechanism for spatiotemporal intermittency is described. It occurs in systems that exhibit bistability between a homogeneous stationary state and an oscillatory one, close to parameter values where the oscillation disappears through an Andronov homoclinic bifurcation. © 1998 Elsevier Science B.V. All rights reserved.

---

## 1. Introduction

Spatiotemporal chaos denotes a complex dynamical behavior which is observed in spatially extended physical systems. From a mathematical point of view, it is associated with a solution of a partial differential equation characterized by a number of positive Lyapunov exponents that increases with the size of the domain. Phase turbulence [1], defect mediated turbulence [2], self-focusing turbulence [3], and spatiotemporal intermittency [4] provide different forms of spatiotemporal chaos. From the theoretical side, little is known about the possible mechanisms leading to spatiotemporal chaos. In this paper, a generic mechanism leading to spatiotemporal intermittency is described. Several models that display this kind of behavior are reviewed in the first part. The second part is devoted to the analysis of a simple model that is based on the normal form of a degenerate bifurcation. Spatiotemporal intermittency appears as a consequence of the bistability between an oscillatory behavior and a stationary state.

Spatiotemporal intermittency has been described in the context of partial differential equations, coupled maps and cellular automatas [4]. Roughly speaking, it is a complex spatiotemporal behavior that involves two phases: a simple one, that describes a so-called laminar state and a complex one, that has been called “turbulent state”. It is reminiscent of the phenomenon of intermittency observed in low dimensional dynamical

---

\* Corresponding author.

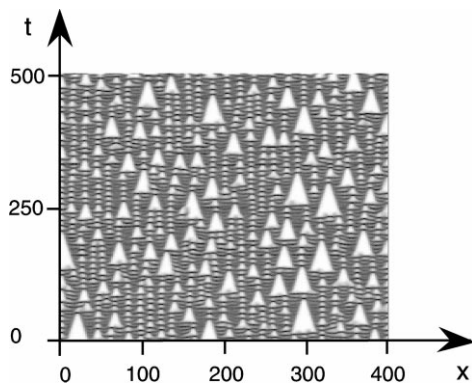


Fig. 1. Typical X–T diagram where spatiotemporal intermittency can be observed. Once laminar state (white color) is nucleated, it disappears due to the propagation of fronts. The dynamical system used here is defined by Eq. (19) and parameter values are:  $a = 2.08$ ,  $\kappa = 1$ , and  $\mu = 0.2$ .

systems [5]. In spatially extended systems, the laminar state is nucleated from the turbulent phase. This laminar state is metastable and disappears through the propagation of fronts (see Fig. 1). In low dimensional dynamical systems, the duration of the laminar phase, close to the onset of intermittency also obeys a simple scaling law [5]. In extended systems, the transition to turbulence is characterized by critical exponents associated with the fraction of turbulent phase into the laminar one.

## 2. Review of some models displaying spatiotemporal intermittency

Spatiotemporal intermittency (see Fig. 1) has been observed in many spatially extended dynamical systems. In the models selected below, numerical and analytical analysis support the idea that this behavior can be understood in the light of a simple mechanism. All these models have the property that near the threshold of the spatiotemporal intermittency, the homogeneous dynamical system (obtained by dropping the spatial derivatives) exhibits bistable properties. The two states in competition are a stable fixed point and a stable limit cycle.

### 2.1. Imperfect Ginzburg–Landau equation

The Ginzburg–Landau equation describing the onset of self-oscillation reads

$$A_t = A - (1 + i\alpha)|A|^2A + (1 + i\beta)A_{xx}, \quad (1)$$

where  $A$  represents the complex amplitude of the oscillation,  $\alpha$  the amplitude-dependent frequency renormalization constant and  $\beta$  measures the dispersion of the waves. This equation possesses many different type of solutions, including waves, defects, and spatiotemporal complex solutions. When the effect of a small periodic forcing with a

frequency close to the natural frequency of the oscillations is taken into account, this equation becomes [6,7]

$$A_t = (1 + i\Omega)A - (1 + i\alpha)|A|^2A + (1 + i\beta)A_{xx} + \gamma, \tag{2}$$

where  $\Omega$  denotes the detuning between the natural and the external frequency and  $\gamma$  the amplitude of the forcing.

Parameter values where spatiotemporal intermittency is observed are the following:  $\gamma = 1.3$ ,  $\alpha = 2$ ,  $\beta = 0.5$ ,  $\Omega = 4.0$ .

### 2.2. The Maxwell–Bloch equation describing a laser to an injected signal

Transverse effects in lasers are described by the Maxwell–Bloch equation where diffraction effects have been included. In the presence of an external electric field with a frequency close to frequency of the laser [8,9], those equations reads

$$\begin{aligned} E_t &= \kappa(P - (1 + i\theta)E) + \mathcal{E} + i\eta E + i\alpha E_{xx}, \\ P_t &= \gamma_{\perp}(\Delta E - (1 - i\theta)P) + i\eta P, \\ \Delta_t &= \gamma_{\parallel}(\Delta_0 - \Delta - \frac{1}{2}(P^*E + PE^*)), \end{aligned} \tag{3}$$

where  $\kappa$ ,  $\gamma_{\perp}$ ,  $\gamma_{\parallel}$  represent the damping constants, respectively, associated with the complex amplitude of the electric field  $E$ , the complex amplitude of polarization  $P$  and the inversion population  $\Delta$ . The parameter  $\theta$  measures the detuning between the atomic frequency and the nearest frequency of the cavity,  $\Delta_0$  the pump,  $\alpha$  the diffraction coefficient,  $\mathcal{E}$  the amplitude of the external signal and  $\eta$  the detuning between the operating laser frequency and the frequency of the injected signal.

Spatiotemporal intermittency is observed with parameters values:  $\kappa = 5$ ,  $\theta = 3$ ,  $\eta = 1.2$ ,  $\gamma_{\perp} = 50$ ,  $\gamma_{\parallel} = 20$ ,  $\Delta_0 = 11$ ,  $\alpha = 0.5$ ,  $\varepsilon = 0.5$ .

### 2.3. Reaction–diffusion equations

The next example is the Gray–Scott model [10]. This model describes a cubic autocatalytic chemical reaction in an open spatial reactor:

$$U_t = 1 - U - \mu UV^2 + \delta U_{xx}, \quad V_t = \mu UV^2 - vV + V_{xx}. \tag{4}$$

Spatiotemporal intermittency appears for  $\mu = 145$ ,  $v = 5$  and  $\delta = 1$ .

### 2.4. An example with a third derivative in time

The following third-order dynamical system is the normal form a codimension three singularity:

$$U_{ttt} + \mu U_{tt} + \nu U_t + U + aU^2 + bU^3 = U_{xxt} + \kappa U_{xxt}. \tag{5}$$

The two coupling terms on the right-hand side equation represents, respectively, diffusion and dispersion effects.

Spatiotemporal intermittency exists when parameters are taken to be  $\mu = 1$ ,  $\nu = 0.445$ ,  $a = 2.01$ ,  $b = 1$ ,  $\kappa = 1$ .

### 2.5. A biochemical model describing seashell patterns

In a work devoted to the modelisation of pigmentation patterns observed on the shell of some tropical mollusc, Meinhardt, and Klingler [11] have introduced the following coupled partial differential equations:

$$\begin{aligned} a_t &= r_a b a_*^2 - r_a + D_a a_{xx}, \\ b_t &= b_b (1 + s_b c + c_b d) - r_a b a_*^2 - r_b b + D_b b_{xx}, \\ c_t &= r_c a \left( \frac{c^2 + b_c}{s_d + d} \right) - r_c c + D_c c_{xx}, \\ d_t &= r_c a (c^2 + b_c) - r_d d + D_d d_{xx}, \end{aligned} \quad (6)$$

where  $a_*^2 = (a^2/1 + s_a a^2) + b_a$ . The two first equations describe the pigmentation reaction (represented an activator–substrate system), whereas the two last ones are associated to an enhancing reaction (represented by an activator–inhibitor system).

Spatiotemporal intermittency occurs for the following parameter values:  $D_a = 0.01$ ,  $D_b = 0.0$ ,  $D_c = 0.2$ ,  $D_d = 0.1$ ,  $r_a = 0.05$ ,  $r_b = 0.0045$ ,  $r_c = 0.1$ ,  $r_d = 0.05$ ,  $b_a = 0.0$ ,  $b_b = 0.0220$ ,  $b_c = 0.02$ ,  $b_d = 0.0$ ,  $s_b = 3$ ,  $s_c = 0.0$ ,  $s_d = 0.01$ .

### 2.6. A model describing a coupled neural network

The model is based on Morris–Lecar model [12]. This system is a simplified version of the Hodgkin–Huxley model [13] with two variables instead of four dynamical system variables in the (HH) model.

$$\begin{aligned} \frac{\partial v}{\partial t} &= -I_{ion}(v, w) + I + \frac{\partial^2 v}{\partial x^2}, \\ \frac{\partial w}{\partial t} &= f \frac{(w_\infty(v) - w)}{\tau_w(v)} \end{aligned} \quad (7)$$

with

$$\begin{aligned} I_{ion} &= \bar{g}_{ca} m_\infty(v)(v - 1) + \bar{g}_K w(v - v_K) + \bar{g}_L (v - v_L), \\ m_\infty(v) &= \frac{1}{2} \left[ 1 + \tanh \left( \frac{v - v_a}{v_b} \right) \right], \end{aligned}$$

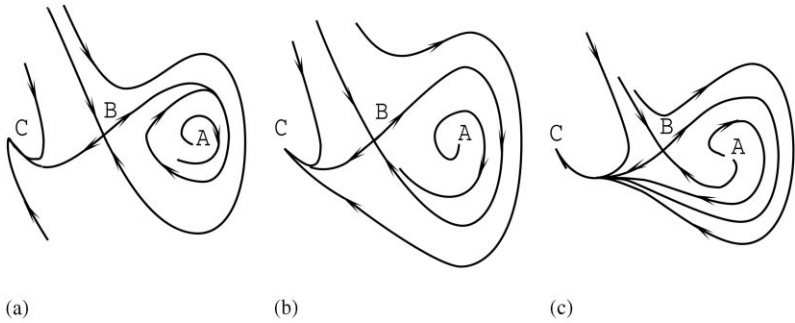


Fig. 2. Typical phase portrait of homogeneous dynamical systems obtained for different parameter values: (a) below the homoclinic bifurcation, there is bistability between the limit cycle and the fixed point; (b) at the threshold, the limit cycle reaches the saddle point; (c) above the bifurcation the stable fixed point becomes the only stable attractor.

$$w_\infty(v) = \frac{1}{2} \left[ 1 + \tanh \left( \frac{v - v_c}{v_d} \right) \right],$$

$$\tau_w(v) = \frac{1}{\cosh \left( \frac{v - v_c}{2v_d} \right)}.$$

This model includes a calcium current generating fast action potentials  $u$  and a delayed rectifier potassium current  $w$ . To maintain a constant potential at a resting rate, a leak current  $I$  is also included. The spatial coupling is insured through the variable  $v$  [14].

Spatiotemporal intermittency is observed with parameter values:  $v_a = -0.01$ ,  $v_b = 0.15$ ,  $v_c = 0.1$ ,  $v_d = 0.145$ ,  $\bar{g}_{ca} = 1.0$ ,  $\bar{g}_K = 2.0$ ,  $\bar{g}_L = 0.5$ ,  $V_k = -0.7$ ,  $v_l = -0.5$ ,  $F = 1.15$ ,  $I = 0.049$ .

### 2.7. A mechanism of intermittency

In the models considered above, spatiotemporal intermittency appears as a robust scenario when one parameter is varied. In the corresponding local dynamical system obtained by dropping the spatial derivatives, this scenario involves bistability between a fixed point and a limit cycle that disappears through a Andronov Homoclinic bifurcation [15,16] close to the threshold of spatiotemporal intermittency. Such a bistable behavior can be pictured in two dimensions (see Fig. 2). When the spatial effects are taken into account, the limit cycle becomes unstable under inhomogeneous perturbations: this instability is related to a self-focusing instability as we will argue later. Owing to this mechanism, the phase coherence of the oscillations is broken. This leads to a form of spatiotemporal disorder [17–20] that acts as an intrinsic noise. Above a parameter value, this “noise” leads to the nucleation of the stationary state. Depending upon the relative stability of the laminar state and the disordered state, the domains nucleated either grow or shrink. In the case where they shrink, i.e. when the stationary

phase is metastable [21], a permanent complex nucleation process occurs. It provides a simple example of spatiotemporal intermittency [22] for models reviewed above. This qualitative picture raises two questions we would like to address in the next section:

- (i) What is the nature of the fronts observed and why do they move in the direction to make the collapse of the laminar phase?
- (ii) What is the mechanism of nucleation of the laminar phase from the turbulent one ?

### 3. A simple model

In order to describe more quantitatively the scenario of the transition to spatiotemporal intermittency, a simpler model is introduced. Since the basic ingredient is the bistability between a fixed point and a limit cycle, it is enough to consider a family of planar dynamical systems.

#### 3.1. Bistability between two stationary phases

The simplest dynamical system that exhibits a bistable behavior between two fixed points reads

$$U_t + \frac{\partial V}{\partial U} = 0, \quad (8)$$

where the Lyapunov function  $V$  has been pictured in Fig. 3 . The simplest analytical expression for this potential  $V$  reads

$$\frac{\partial V}{\partial U} = \alpha + \beta U + \gamma U^2 + \delta U^3 .$$

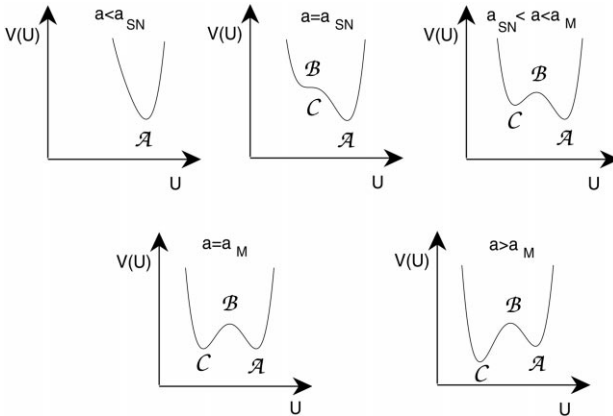


Fig. 3. Typical function  $V(U)$  obtained for a different set of parameters.

A further simplification occurs if one assumes that  $U = 0$  is a stationary solution. In that case  $V$  is given by

$$\frac{\partial V}{\partial U} = \beta U + \gamma U^2 + \delta U^3.$$

Obvious scalings allow us to study a one-parameter family of dynamical systems

$$U_t + U + aU^2 + U^3 = 0, \tag{9}$$

where the sign of the linear and the cubic terms have been chosen for stability considerations. In the range of parameter  $a_{SN} < a < a_M$ , Eq. (9) possesses three stationary solutions:  $U = 0$ ,  $U = -a/2 + (\sqrt{\Delta}/2)$ ,  $U = -a/2 - (\sqrt{\Delta}/2)$ , respectively noted  $\mathcal{A}$ ,  $\mathcal{B}$ , and  $\mathcal{C}$  (See Fig. 3), where  $\Delta = a^2 - 4$ . The notation  $a_{SN} = 2$  stands for the value of  $a$  at which  $\mathcal{B}$  and  $\mathcal{C}$  disappear through a saddle node bifurcation (spinodal point in the language of phase transition) and  $a_M = 3\sqrt{2}/2 \simeq 2.12132$  stands for the value at which  $V_{\mathcal{A}} = V_{\mathcal{C}}$  (the Maxwell point of the potential  $V$  in phase transition terminology). Eq. (9) is actually a normal form of the pitchfork bifurcation, in the presence of an imperfection, under the assumption of the persistence of the trivial solution  $U = 0$ . Without noise, the question of the relative stability of the two stable fixed points  $\mathcal{A}$  and  $\mathcal{C}$  is irrelevant. The spatial extension of Eq. (9) is obvious. It reads

$$U_t + U + aU^2 + U^3 = U_{xx}, \tag{10}$$

where the diffusion coefficient has been chosen to unity by a proper choice of the space variable. The diffusion term appears as the simplest linear term which leads to a spatial coupling, that preserves the reflection symmetry of the space variable  $x$  and the translational symmetry. This partial differential equation is an infinite-dimensional gradient flow which can be written as

$$U_t + \frac{\partial \mathcal{V}}{\partial U} = 0, \tag{11}$$

where the functional  $\mathcal{V}$  reads

$$\mathcal{V} = \int_{-\infty}^{\infty} \left( V(U) + \frac{1}{2} U_x^2 \right) dx.$$

The functional form of Eq. (11) implies that asymptotic solutions of Eq. (11) are stationary. Nevertheless, in the bistable regime  $a > a_{SN}$ , moving fronts that connect asymptotically in space  $\mathcal{A}$  and  $\mathcal{C}$  do exist. Their velocities can be used to define the relative stability of the two stationary phases [21]. A solution  $U_{\mathcal{A}\mathcal{C}}(x - c_{\mathcal{A}\mathcal{C}}t)$  of Eq. (10) obeys the equation

$$\ddot{U}_{\mathcal{A}\mathcal{C}} + c_{\mathcal{A}\mathcal{C}} \dot{U}_{\mathcal{A}\mathcal{C}} + \frac{\partial W}{\partial U_{\mathcal{A}\mathcal{C}}} = 0, \tag{12}$$

where  $W = -V$  and the dot denotes the derivative by respect to  $\zeta = x - c_{\mathcal{A}\mathcal{C}}t$ . Eq. (12) corresponds to a nonlinear eigenvalue problem since  $U_{\mathcal{A}\mathcal{C}}$  and  $c_{\mathcal{A}\mathcal{C}}$  are both unknown. The boundary conditions are  $U_{\mathcal{A}\mathcal{C}}(-\infty) = U_{\mathcal{A}} = 0$  and  $U_{\mathcal{A}\mathcal{C}}(+\infty) = U_{\mathcal{C}} = -a/2 - (\sqrt{\Delta}/2)$ . Multiplying Eq. (12) by  $\dot{U}_{\mathcal{A}\mathcal{C}}$  and integrating over  $\zeta$  allows us to get the relation

$$c_{\mathcal{A}\mathcal{C}} = \frac{V_{\mathcal{C}} - V_{\mathcal{A}}}{\int (\dot{U}_{\mathcal{A}\mathcal{C}})^2 d\zeta}. \quad (13)$$

We have used the following asymptotic property of the front:  $\dot{U}_{\mathcal{A}\mathcal{C}}(\pm\infty) = 0$  in order to obtain this formula. The velocity of the front is thus proportional to  $V_{\mathcal{C}} - V_{\mathcal{A}}$ . This criterion is consistent with the intuition that if  $V_{\mathcal{C}} > V_{\mathcal{A}}$ , then the phase  $\mathcal{C}$  is metastable. This defines a metastability criterion for extended systems, in the absence of noise [21]. An explicit solution to this problem can be obtained close to the Maxwell point where fronts becomes static interfaces separating domains characterized by the same “potential energy”. At the Maxwell point a solution is given by

$$U_{\mathcal{A}\mathcal{C}} = -\frac{\sqrt{2}}{2} \left( 1 + \tanh\left(\frac{x}{2}\right) \right). \quad (14)$$

When  $a = a_M + \varepsilon$ , one obtains the explicit formula for the front velocity,

$$c_{\mathcal{A}\mathcal{C}} = -2\sqrt{2}\varepsilon.$$

We next generalize this model in order to allow for the existence of a limit cycle.

### 3.2. Bistability between a stationary and an oscillatory phase

The simple model for describing oscillations is provided by the normal form of the Andronov–Hopf bifurcation (see Eq. (1)). Unfortunately, this model does not display bistability between a limit cycle and a fixed point. Although the imperfect Ginzburg–Landau equation (2) possesses this property, it is too complicated for a detailed analytical study. Another candidate is the quintic Ginzburg–Landau equation introduced by Thual and Fauve [23] in order to study localized non-equilibrium solutions. We ruled out this model because it corresponds to a different type of bistability, in which the separatrix is provided by an unstable limit cycle. This is not the type of bistability which has been numerically observed in the models discussed previously. The Andronov–Hopf bifurcation in the singular limit where the oscillation occurs at low frequency is actually the straightforward generalization of the problem considered previously. From a mathematical point of view this bifurcation is known as the Bogdanov–Takens bifurcation [24] with the reflection symmetry  $U \rightarrow -U$ , in the presence of an imperfection which preserves the stationary solution  $U = 0$ ,

$$U_{tt} + \mu_1 U_t + \varepsilon_1 U U_t + \alpha U^2 U_t + \mu_2 U + \varepsilon_2 U^2 + \beta U^3 = 0, \quad (15)$$

where  $\varepsilon_1$ ,  $\varepsilon_2$  measure the effects of the imperfection,  $\mu_1$ ,  $\mu_2$  the unfolding parameters of the linear problem and  $\alpha$ ,  $\beta$  are order unity parameters. In order to insure the existence

of bounded solutions  $\alpha$  and  $\beta$  are assumed to be positive. It is useful to write this equation into the following way:

$$U_{tt} + v(U)U_t + \frac{\partial V}{\partial U} = 0, \tag{16}$$

where

$$v(U) = \mu_1 + \varepsilon_1 U + \alpha U^2$$

and

$$V = \frac{1}{2}\mu_2 U + \frac{1}{3}\varepsilon_2 U^2 + \frac{1}{4}\beta U^3.$$

Scale changes allow us to reduce the number of parameters from 6 to 4. It is enough to consider the two-parameters family obtained by choosing  $\mu_1 = -\mu$ ,  $\varepsilon_1 = 0$ ,  $\alpha = 1$ ,  $\mu_2 = 1$ ,  $\varepsilon_2 = a$  and  $\beta = 1$ .

$$v(U) = -\mu + U^2.$$

and  $V$  reduces to the potential considered in the previous section. Eq. (16) is a particular form of the Van der-Pol–Duffing equation. For negative  $\mu$ , in the bistable regime, Eq. (16) possesses two stable fixed points  $\mathcal{A}$  and  $\mathcal{C}$  and a saddle fixed point  $\mathcal{B}$ . The stable manifold of this point is the separatrix. For  $\mu = 0$ , the fixed point  $\mathcal{A}$  becomes unstable through a supercritical Andronov–Hopf bifurcation. For  $\mu$  slightly positive, the Eq. 16 reduces to the Landau equation

$$A_\tau = \mu A - (1 + i\alpha)|A|^2 A, \tag{17}$$

where  $\alpha = (10a^2/3) - 3$ ,  $U = Ae^{it} + \bar{A}e^{-it} - 2a|A|^2 + (a/3)(A^2e^{2it} + \bar{A}^2e^{-2it}) + h.o.t.$  and  $\tau = \frac{t}{2}$ . When  $\mu$  increases to a critical value  $\mu_A$ , a second bifurcation occurs in which the limit cycle disappears on the saddle point  $\mathcal{B}$  through an Andronov-homoclinic bifurcation. Slightly above this value,  $\mathcal{C}$  is the unique attractor of the dynamical system. An analytical calculation of this value is possible close to the Maxwell point, since there, the Eq. 16 appears to be a perturbation of an Hamiltonian system whose solutions are known analytically:

$$U_{tt} + \frac{\partial V}{\partial U} = 0. \tag{18}$$

One obtains  $\mu_A = (9/10 - 3\pi\sqrt{2}/16)\varepsilon$ , where  $a = a_M + \varepsilon$ . Bifurcations occurring for larger  $\mu$  play no role for studying the spatiotemporal intermittency. The scenario, we are interested to describe when spatial coupling is included, is the following: in the parameter regime where  $a_{SN} < a < a_M$ , i.e. when bistability occurs and when  $\mathcal{C}$  is metastable in the usual sense, we increase  $\mu$  from zero to  $\mu_A$ . Starting with an initial condition close to the fixed point  $\mathcal{A}$ , we first observe its instability which leads to a limit cycle, which in turn disappears through an homoclinic bifurcation where its period diverges.

For bigger values of  $\mu$ , the dynamical system possesses just one attractor: the stable fixed point  $\mathcal{C}$ . This simple scenario is strongly affected by spatial coupling effects. The “spatial unfolding” of the Bogdanov–Takens normal form is given by

$$U_t + v(U)U_t + \frac{\partial V}{\partial U} = U_{xx} + \kappa U_{xt}. \quad (19)$$

The terms on the right-hand side of Eq. (19) represent, respectively, the propagation and diffusion effects. We first address the question of the front solution which separates the  $\mathcal{A}$  from the  $\mathcal{C}$  phase. Because the phase  $\mathcal{C}$  is metastable, the front moves with a velocity  $c_{\mathcal{A}\mathcal{C}}$  and obeys the following equation:

$$c_{\mathcal{A}\mathcal{C}}\kappa F_{\zeta\zeta\zeta} + (c_{\mathcal{A}\mathcal{C}}^2 - 1)F_{\zeta\zeta} - c_{\mathcal{A}\mathcal{C}}v(F)F_{\zeta} + \frac{\partial V}{\partial F} = 0, \quad (20)$$

where  $F$  is the front in the moving frame,  $\zeta = x - c_{\mathcal{A}\mathcal{C}}t$  and  $F(-\infty) = U_{\mathcal{A}} = 0$ ,  $F(+\infty) = U_{\mathcal{C}} = -a/2 - (\sqrt{A}/2)$ . For large negative values of  $\mu$ , it is easy to prove the existence of such a front since Eq. (19) then reduces at the leading order to Eq. (10), where  $t$  is replaced by  $t/-\mu$ . We do conjecture that such a solution exists for any negative  $\mu$  and even for a range of positive value of this parameter. Our argument is based upon a numerical resolution of Eq. (20) using a variant of the shooting method. Assuming the existence of such a solution, one gets the following expression for the velocity:

$$c_{\mathcal{A}\mathcal{C}} = \frac{V_{\mathcal{C}} - V_{\mathcal{A}}}{\int v(F)(\partial_{\zeta}F)^2 d\zeta - \kappa \int \partial_{\zeta\zeta}F \partial_{\zeta}F d\zeta}, \quad (21)$$

which, as far as its denominator is positive, leads to the usual metastability criterion. For  $\mu$  small enough, its positivity is guaranteed. At the Maxwell point, the front that becomes a static interface does exist for any value of  $\mu$ . Close to the Maxwell point and for small values of  $\mu$ , the front moves slowly and can be explicitly constructed in perturbation of  $\varepsilon = a_M - a$ . The explicit formula for the velocity is then given by

$$c_{\mathcal{A}\mathcal{C}} = \frac{10\sqrt{2}}{3 + \kappa - 5\mu}\varepsilon. \quad (22)$$

The perturbative expansion, valid for  $\varepsilon$  and  $\mu$  small, breaks down before the critical value of  $\mu$  where the velocity diverges  $\mu_c = (3 + \kappa/5)$ . This gives the indication that the front can exist for a range of positive  $\mu$ . It is confirmed by computing this velocity using a shooting method (see Fig. 4). For positive values of  $\mu$ , this front is unstable, since the  $\mathcal{A}$  phase itself is unstable. The stability of the  $\mathcal{A}$  phase is straightforward. Close to the birth of the oscillations ( $\mu \simeq 0$ ), Eq. (19) can be reduced to the complex Ginzburg–Landau equation (1) for the complex amplitude of the homogeneous oscillations, using standard asymptotic methods [18,1]:

$$A_{\tau} = \mu A - (1 + i\alpha)|A|^2 A + (1 + i\beta)A_{xx}, \quad (23)$$

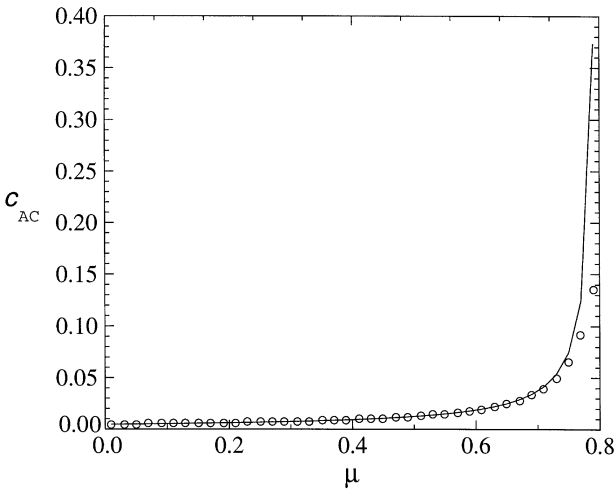


Fig. 4. Plot of the front velocity near the Maxwell point ( $a_M - a = 10^{-3}$ ) as a function of the parameter  $\mu$ . The solid line represents analytical computation of  $c_{\mathcal{A}\mathcal{C}}$  (22) and the dots numerical computation through a shooting method.

where  $\alpha = (10a^2/3) - 3$ ,  $\beta = -1$ ,  $\tau = t/2$ ,  $\kappa$  has been chosen equal to the unity for the sake of simplicity and

$$U = Ae^{it} + \bar{A}e^{-it} - 2a|A|^2 + \frac{a}{3}(A^2e^{2it} + \bar{A}^2e^{-2it}) + \dots \quad (24)$$

The homogeneous limit cycle oscillates with a non-zero mean value which is consistent with the asymmetry of the “potential”  $V$ . When  $a = 0$ , the Benjamin–Feir criterion ( $1 + \alpha\beta > 0$ ) for the stability of the homogeneous oscillations  $A = \sqrt{\mu}e^{-i\alpha\mu\tau}$  is satisfied. The self focusing instability occurs for  $a \simeq 1.095$ . It takes place before the saddle node bifurcation leading to the appearance of homogeneous solutions  $\mathcal{B}$  and  $\mathcal{C}$ . In the bistable regime, for small  $\mu$ , we first observe phase and defect turbulence [2,25]. For larger  $\mu$ , self focusing becomes stronger. The following numerical experiment is performed. We start from a noisy initial condition close to the stationary solution  $\mathcal{A}$ , we choose a typical value of  $a = 2.08$  in the bistable regime such that  $V_{\mathcal{A}} < V_{\mathcal{C}}$ , and we increase the parameter  $\mu$ . Close to a critical value  $\mu = 0.12$ , where the limit cycle has already disappeared ( $\mu_A \simeq 0.0761$ ), the first nucleation events of the  $\mathcal{C}$  phase are observed. In this regime of parameters, we observe self focusing and defect mediated turbulence [2]. The presence of the defects, where the oscillation vanishes, reduces the mean square value of the fluctuations. This accounts for the parameter shift between the nucleation transition and the homoclinic bifurcation. A precise numerical computation of this mean square value allows us to get a good quantitative estimate of the nucleation threshold. The domains of state  $\mathcal{C}$  (the white triangle in Fig. 1), once nucleated, retract almost uniformly in time with the velocity  $c \simeq 0.210$ , for  $\mu \simeq 0.2$ . The fronts observed numerically separate the turbulent phase from the  $\mathcal{C}$  phase. The velocity of this front that connects the turbulent state and  $\mathcal{C}$  may be computed by performing the

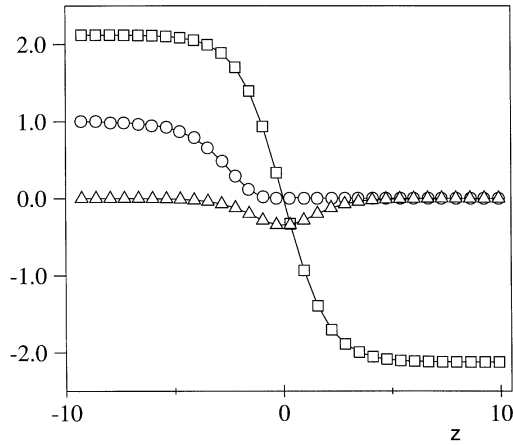


Fig. 5. Plot of the functions  $(\Delta) \partial U_{\mathcal{A}\mathcal{C}}/\partial z$ ,  $(o) |\chi|^2$ ,  $(\diamond) \frac{1}{2} \partial^3 V/\partial U^3$ .

bifurcation analysis of the weakly unstable front which connects  $\mathcal{A}$  to  $\mathcal{C}$ , close to the Maxwell point, and  $\mu \simeq 0$ . When  $V_{\mathcal{A}} = V_{\mathcal{C}}$ , the front which connects  $\mathcal{A}$  to  $\mathcal{C}$  is stationary and reads

$$U_{\mathcal{A}-\mathcal{C}} = -\frac{\sqrt{2}}{2} \left( 1 + \tanh \left( \frac{x-p}{2} \right) \right), \tag{25}$$

where  $p$  represents the arbitrary position of the domain wall. For slightly positive  $\mu$ , this solution is unstable because  $\mathcal{A}$  itself is unstable. As usual [26], this instability couples to the translation degree of freedom of the domain wall, and leads to its propagation. The velocity of the perturbed front is found, as a solvability condition, by looking for solutions of Eq. (19) in the form  $U(x, t) = U_{\mathcal{A}-\mathcal{C}}(x - p) + W$ . One gets

$$\frac{\partial p}{\partial t} = C_{eq} + C_{neq}, \tag{26}$$

where

$$C_{eq} = \frac{5\sqrt{2}}{2} (a_M - a),$$

$$C_{neq} = \frac{15}{4} \int_{-\infty}^{\infty} |\chi|^2 |A|^2 \partial_{\zeta} U_{\mathcal{A}-\mathcal{C}} \left. \frac{\partial^3 V}{\partial U^3} \right|_{U=U_{\mathcal{A}-\mathcal{C}}} d\zeta \tag{27}$$

and  $W = A\chi e^{it} + c.c. + h.o.t.$  (see Fig. 5). Here  $\chi$  represents the most unstable eigenfunction of the front solution. It obeys the equation  $L(\zeta)\chi = 0$ , where,

$$L = \frac{\partial^2}{\partial \zeta^2} - \frac{(1-i)}{2} U(2a + (3+i)U_{\mathcal{A}-\mathcal{C}}) \tag{28}$$

and  $\partial \chi / \partial x = 0$  at the boundaries. The complex envelop of the oscillations is noted as  $A$  and whose dynamics, determined at next order, is described by a generalization

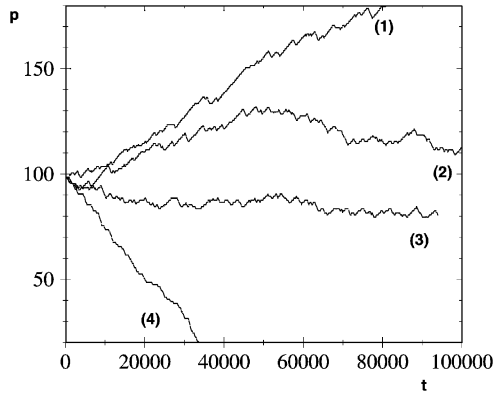


Fig. 6. Position of the interface as a function of the time for different values of parameter  $a$ .  $\mu$  is taken to be 0.05. (1)  $a = 2.1205$ ; (2)  $a = 2.1206$ ; (3)  $a = 2.1207$ ; (4)  $a = a_M = 2.12132$ .

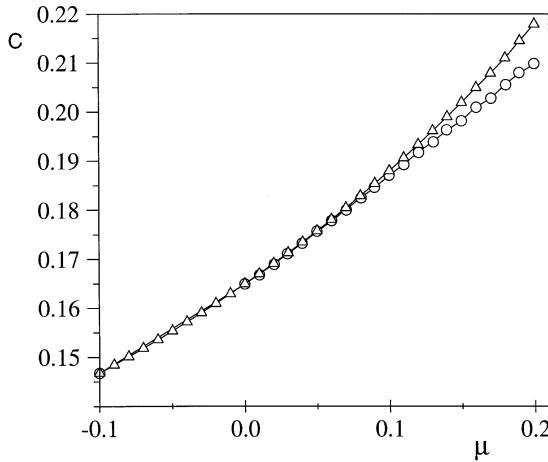


Fig. 7. Velocity of the fronts as functions of  $\mu$ , for  $a = 2.08$ . ( $\Delta$ ) Velocity of the unstable front that connects  $\mathcal{C}$  to  $\mathcal{A}$ , (0) averaged velocity of turbulent front.

of the complex Ginzburg–Landau equation. The first term  $C_{eq}$  in Eq. (26) represents the shift in velocity observed for the domain wall induced by the relative change of the stability of the states  $\mathcal{A}$  and  $\mathcal{C}$  associated with the “potential”  $V$ . The second term  $C_{neq}$ , is associated with the supercritical instability of the  $\mathcal{A}$  state. Owing to the Benjamin–Feir–Newell instability [1,18],  $A$  is fluctuating. This term can be split into two parts: a constant part defined by its temporal mean value  $\langle C_{neq} \rangle$ , and a zero mean value fluctuating part. The constant shift leads to a small correction to the Maxwell condition, obviously related to the asymmetry of the oscillations (see Fig. 6). It is, as expected from symmetry consideration ( $A \rightarrow Ae^{i\phi}$  and  $t \rightarrow t + \phi$ ), a function of  $|A|^2$  only. Although, this formula does not apply for parameter values where the nucleation

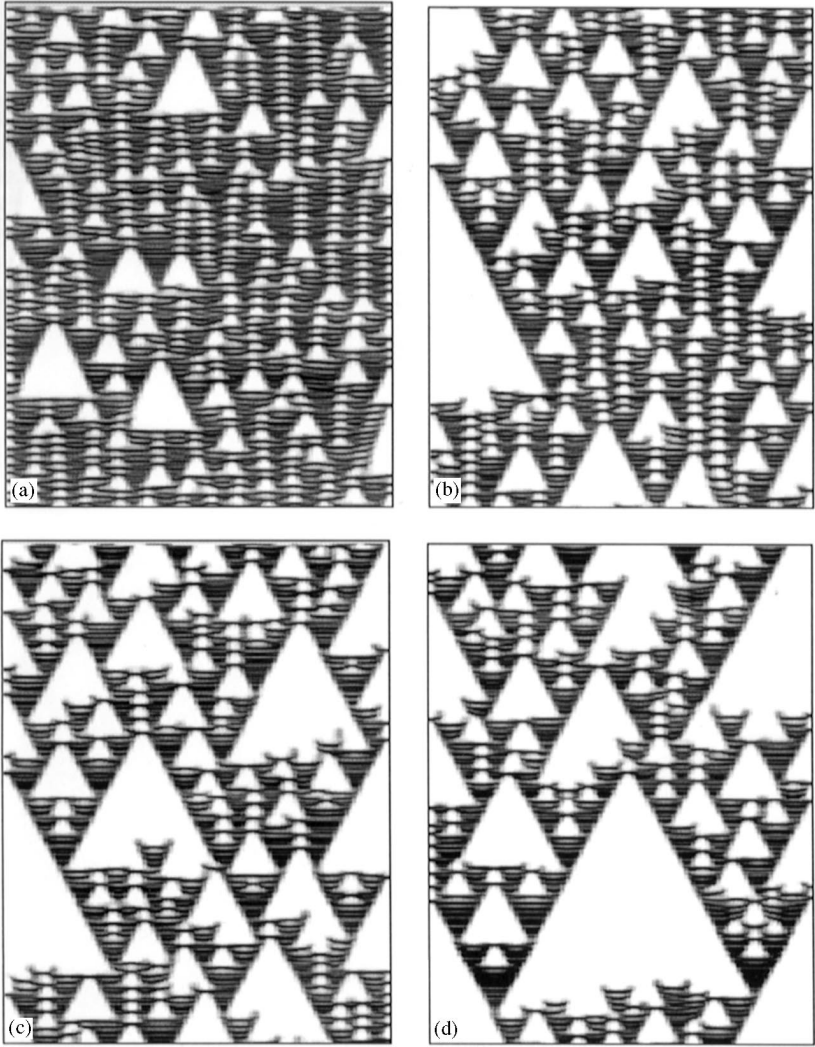


Fig. 8. X–T diagrams obtained for different values of  $\mu$  showing the transition from a turbulent state to a laminar one through spatiotemporal intermittency. Time is running up, the size of the box is 400 and  $a = 2.08$ . The white color represents the laminar domains. (a)  $\mu = 0.2$ ; (b)  $\mu = 0.25$ ; (c)  $\mu = 0.27$ ; (d)  $\mu = 0.275$ .

takes place, it gives a correct qualitative interpretation of the front motion. The front which connects  $\mathcal{C}$  to the chaotic oscillations can be approximated, close to the core of the interface, as a perturbation of the unstable front  $U_{\mathcal{A}-\mathcal{C}}$  which connects  $\mathcal{A}$  to  $\mathcal{C}$ . This front and its velocity have been computed numerically by a shooting method allowing to find a heteroclinic solution of the equation

$$cU_{\xi\xi\xi} + (c^2 - 1)U_{\xi\xi} - cv(U)U_{\xi} + \frac{\partial V}{\partial U} = 0. \quad (29)$$

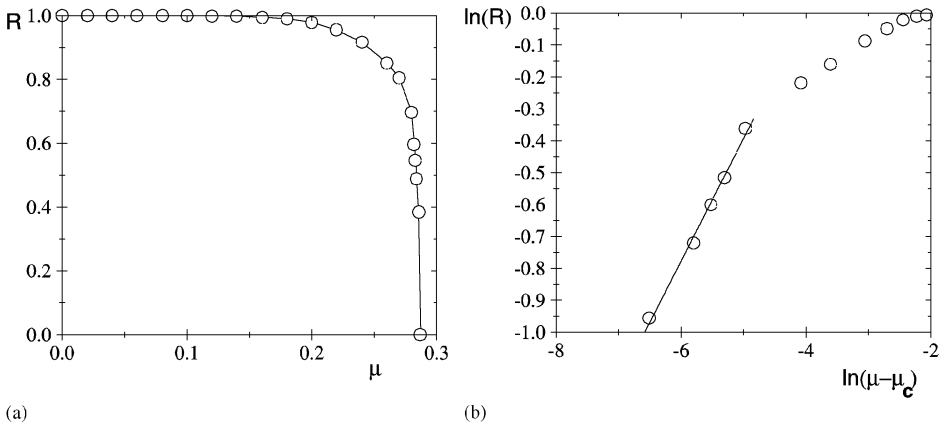


Fig. 9. Transition from turbulent state to stationary one. (a) Plot of the mean value of the turbulent fraction  $R$  for  $a = 2.08$ . (b) Log–Log representation of  $R$  that shows a critical exponent  $(\mu - \mu_c)^\beta$ , with  $\beta = 0.38 \pm 0.02$ . The box's width is 100 000, and the interval of time is more than 100 000 units of time.

The velocity of the actual interface can be obtained by a formula analogous to Eq. (6), where  $C_{eq}$  becomes the velocity of the unstable front  $U_{sd-\mathcal{C}}$ . Fig. 7 shows the difference between the velocity of the interface  $U_{sd-\mathcal{C}}$  and the actual front. Close to  $\mu \geq 0$ , for a finite range of parameter, the instability is convective [27]. Consequently, there is no difference between the two velocities. When the instability becomes absolute, the contribution of the instability to the front motion becomes evident. The behavior of the solutions when  $0.12 < \mu < 0.28$  in which the chaotic nucleation of the metastable phase  $\mathcal{C}$  is observed presents statistical properties similar to those of spatiotemporal intermittency [22] (see Fig. 1). As  $\mu$  is increased, the size of the domains nucleated increases (see Fig. 8) up to a critical value of  $\mu$  where turbulent state no longer exists. Thus, the fraction of “turbulent” state  $R$  decreases from 1.0 to 0.0, where the metastable phase “percolates” (see Fig. 9).

We have described in this letter a spatiotemporal complex state which consists in the nucleation of metastable domains. The mechanism underlying this deterministic “cavitation process” is intimately related to the modulational instability of the oscillation induced by the bistability. Close to the “Maxwell point  $a_M$ ”, “robust localized states” whose nature is different from those related to a subcritical Hopf bifurcation [23], are observed. Close to the spinodal point where the  $\mathcal{B}$  and  $\mathcal{C}$  disappear through a saddle node bifurcation, excitable waves are observed. The parameter range of their stabilities is particularly interesting. On one side, it is bounded by a transition from excitation to oscillation [28] and on the other side, by an instability of the excitable waves which leads to back emission of propagating pulses [29]. Owing to the existence of an analogue of surface tension, in two space dimensions, the nucleated domains, take the form of circular bubbles which eventually retract self similarly in time.

This work has been partially supported by the E.E.C contract number CT93-0107 and CT96-010.

## References

- [1] Y. Kuramoto, *Chemical Oscillations, Waves, and Turbulence*, Springer, Berlin, 1984.
- [2] B.I. Shraiman, *Phys. Rev. Lett.* 57 (1986) 325. See also P. Coulet, L. Gil, J. Lega, *Phys. Rev. Lett.* 62 (1989) 1619.
- [3] A.C. Newell, D.A. Rand, D. Russel, *Physica D* 33 (1988) 281.
- [4] H. Chaté, *Transition vers la turbulence via intermittence spatio-temporelle*, Ph.D. Thesis, University Pierre et Marie Curie, Paris, 1989.
- [5] Y. Pomeau, P. Manneville, *Commun. Math. Phys.* 74 (1980) 189–197.
- [6] J.M. Gambaudo, *J. Differential Equations* 57 (1985) 172.
- [7] P. Coulet, K. Emilsson, *Physica D* 61 (1992) 119–131.
- [8] L.A. Lugiato, L.M. Narducci, D.K. Bandy, C.A. Pennise, *Opt. Commun.* 46 (1983) 64.
- [9] H.G. Solari, G.L. Oppo, *Opt. Commun.* 111 (1994) 173.
- [10] J.H. Merkin, V. Petrov, S.K. Scott, K. Showalter, *Phys. Rev. Lett.* 76 (1996) 546.
- [11] H. Meinhardt, M. Klinger, *J. Theor. Biol.* 126 (1987) 63–89.
- [12] C. Morris, H. Lecar, *Biosphys. J.* 35 (1981) 193.
- [13] A.L. Hodgkin, A.F. Huxley, *J. Physiol. London* 117 (1952) 500.
- [14] S.K. Han, C. Kurrer, Y. Kuramoto, *Int. J. Bifurcation chaos* 7 (4) (1997) 877.
- [15] A.A. Andronov, E.A. Leontovitch, I.I. Gordon, A.G. Maier, *Qualitative theory of second order dynamical systems*, Wiley, New York, 1973.
- [16] A.A. Andronov, in: *Sobraniye Trudov*, A.A. Andronov, Izd. A.N. SSSR, 1956; see also S-N. Chow, C. Liand, D. Wang, *Normal forms and bifurcation of planar vector fields*, Cambridge University Press, Cambridge, 1995.
- [17] T.B. Benjamin, J.E. Feir, *J. Fluid. Mech.* 27 (1967) 417.
- [18] A.C. Newell, *Lect. Appl. Math.* 15 (1974) 157.
- [19] J.T. Stuart, R.C. DiPrima, *Proc. Soc. (London) A* 362 (1978) 27.
- [20] T. Yamada, Y. Kuramoto, *Prog. Theor. Phys.* 56 (1976) 681.
- [21] Y. Pomeau, *Physica D* 23 (1986) 3.
- [22] H. Chaté, P. Manneville, *Phys. Rev. Lett.* 58 (1987) 112.
- [23] O. Thual, S. Fauve, *J. Phys. (Paris)*, 49 (1988) 1820.
- [24] J. Guckenheimer, P. Holmes, *Nonlinear Oscillations, Dynamical Systems and Bifurcation of Vector Fields*. *Appl. Math. Sci.*, Vol. 41, Springer, New York, 1983.
- [25] B.I. Shraiman et al., *Physica D* 57 (1992) 3.
- [26] P. Coulet, G. Iooss, *Phys. Rev. Lett.* 64 (1990) 866. See also G. Iooss, M. Adelmeyer, *Topics in Bifurcation Theory and Applications*, Adv. Ser. in Nonlinear Dynamics, Vol. 3, World Scientific, Singapore, 1992.
- [27] L.D. Landau, E.M. Lifshitz, *Fluid Mechanics*, Pergamon Oxford, 1959.
- [28] M. Argentina, P. Coulet, M. Mahadevan, *Phys. Rev. Lett.* 79 (1997) 2803.
- [29] P. Kanastek et al., *Physica D* 85 (1995) 1 and 2.